Molecular Logic of Prokaryotic Surface Layer Structures

Tanmay A.M. Bharat,[1,2,*] Andriko von Kügelgen,[1,2] and Vikram Alva[3,*]

Most prokaryotic cells are encased in a surface layer (S-layer) consisting of a paracrystalline array of repeating lattice-forming proteins. S-layer proteins populate a vast and diverse sequence space, performing disparate functions in prokaryotic cells, including cellular defense, cell-shape maintenance, and regulation of import and export of materials. This article highlights recent advances in the understanding of S-layer structure and assembly, made possible by rapidly evolving structural and cell biology methods. We underscore shared assembly principles revealed by recent work and discuss a common molecular framework that may be used to understand the structural organization of S-layer proteins across bacteria and archaea.

The S-layer Constitutes the Outermost Shell of Most Prokaryotic Cells

All living cells must interact with their environment to obtain nutrients, find ecological niches for growth, and defend against extracellular attack by predators or viruses. Cellular interaction with the environment is shaped by molecules on the cell surface that detect stimuli and mediate an appropriate cellular response. This need for specialized cell-surface molecules is particularly crucial for prokaryotes [1] because these molecules can enable cellular motility, initiate cellular adhesion to surfaces [2], mediate biofilm formation [3], and regulate the transport of molecules.

The outermost surface of most bacteria, and nearly all archaea, is composed of a 2D sheet of repeating surface-layer proteins or glycoproteins, known as an S-layer. Although the function of S-layers in many organisms has not been experimentally verified, S-layers are known to regulate cell shape, co-ordinate cellular contact with the environment, and act as a barrier protecting prokaryotic cells from predators or phages [4,5]. In human pathogens, such as *Clostridium difficile*, *Bacillus anthracis*, and *Campylobacter fetus*, S-layers play a key role in bacterial infections, and in some cases, such as in *B. anthracis*, the loss or disruption of the (Sap) S-layer renders the bacteria completely avirulent in mouse infection models [6–9]. Due to their high copy numbers, it has been estimated that S-layer proteins, as a group, are one of the most abundant protein families on earth [10].

Due to their striking appearance under the microscope, S-layers have been the subject of inquiry for many eminent structural biologists in the past [11,12]; however, structural and cell biology information on S-layers has been scarce until recently. This is partly due to the lack of suitable methods to study these flexible 2D arrays on cells, and perhaps also due to the absence of S-layers in the common prokaryotic model organisms such as *Escherichia coli* and *Bacillus subtilis*. In the last 3 years there has been renewed interest in the field, with a spate of structural biology, cell biology, and functional genetics studies being published on this topic. In this article we summarize recent work in the light of past information available on S-layers and suggest a molecular framework for understanding S-layer sequence, structure, arrangement, and assembly principles on prokaryotic cells.

Highlights

Despite enormous sequence diversity in surface (S)-layer proteins, structural diversity is much lower than previously thought.

S-layer proteins have a bipartite arrangement with a lattice-forming and an anchoring segment.

Novel structural biology methods are revealing the architectures of S-layers *in situ*.

S-layer assembly across prokaryotes is tightly coupled to the cell cycle, including the cell division machinery.

[1]Sir William Dunn School of Pathology, University of Oxford, Oxford OX1 3RE, UK
[2]Central Oxford Structural Microscopy and Imaging Centre, University of Oxford, Oxford OX1 3RE, UK
[3]Department of Protein Evolution, Max Planck Institute for Developmental Biology, Max-Planck-Ring 5, Tübingen 72076, Germany

*Correspondence:
tanmay.bharat@path.ox.ac.uk (T.A.M. Bharat) and
vikram.alva@tuebingen.mpg.de (V. Alva).

## The Sequence Space of Archaeal and Bacterial S-layer Proteins

S-layers are typically composed of a single, or occasionally two or more, species of usually self-assembling extracellular proteins referred to as surface-layer proteins (SLPs) [5,13,14]. These proteins are highly enriched in hydrophobic and acidic amino acid residues and have chain lengths in the range of about 400 to 2500 amino acid residues. Despite similarities in amino acid composition, SLPs exhibit tremendous sequence diversity (Figures 1 and 2) and often share no or minimal similarity at the sequence level, suggesting multiple independent evolutionary origins for them. While sequence similarity between archaeal and bacterial SLPs is rare, high similarity is generally limited to SLPs of closely related organisms (Figures 1 and 2). However, frequently, even SLPs of closely related organisms, such as those of the bacterial genus *Lactobacillus*, display low or undetectable sequence similarities [15].

Despite exhibiting enormous diversity in sequence and length, most hitherto characterized SLPs share a bipartite architecture, comprising a large segment, involved in 2D lattice formation, often in a metal-ion-dependent manner [11,16–19], and a smaller segment, involved in anchoring to the cell envelope [20–22]. A threonine-rich, intrinsically disordered region separates these two
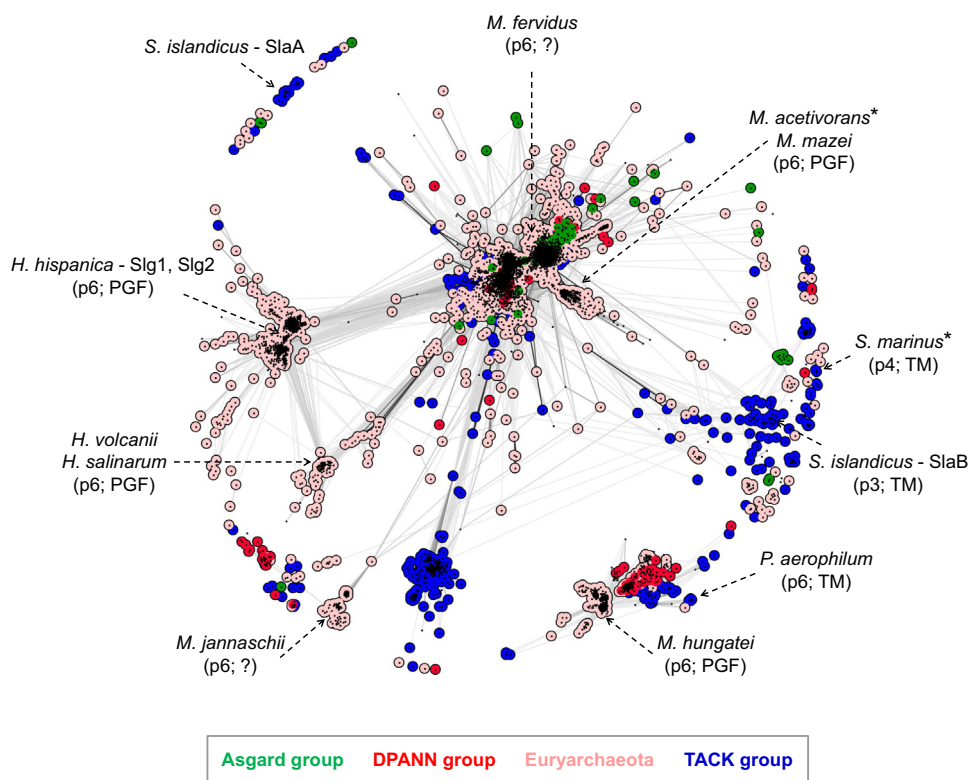
Figure 1. Cluster Map of Archaeal S-layer Proteins. Archaeal S-layer proteins were gathered using BLAST [76] searches and clustered using the CLANS software [77] based on their all-against-all pairwise similarities as measured by BLAST *P* values. Dots represent surface-layer protein (SLP) sequences, and line coloring reflects BLAST *P* values; the darker a line, the lower the *P* value. Colors denote prominent groups of archaea, shown in the box below the map. Some intensely studied archaeal species are highlighted, with the lattice symmetry and predicted anchoring sequence shown in brackets (*denotes S-layers with some structural biology data available). Abbreviations: *H. hispanica*, *Haloarcula hispanica*; *H. salinarum*, *Halobacterium salinarum*; *H. volcanii*, *Haloferax volcanii*; *M. acetivorans*, *Methanosarcina acetivorans*; *M. fervidus*, *Methanothermus fervidus*; *M. hungatei*, *Methanospirillum hungatei*; *M. jannaschii*, *Methanocaldococcus jannaschii*; *P. aerophilum*, *Pyrobaculum aerophilum*; *S. islandicus*, *Sulfolobus islandicus*; *S. marinus*, *Staphylothermus marinus*; TM, transmembrane helix.
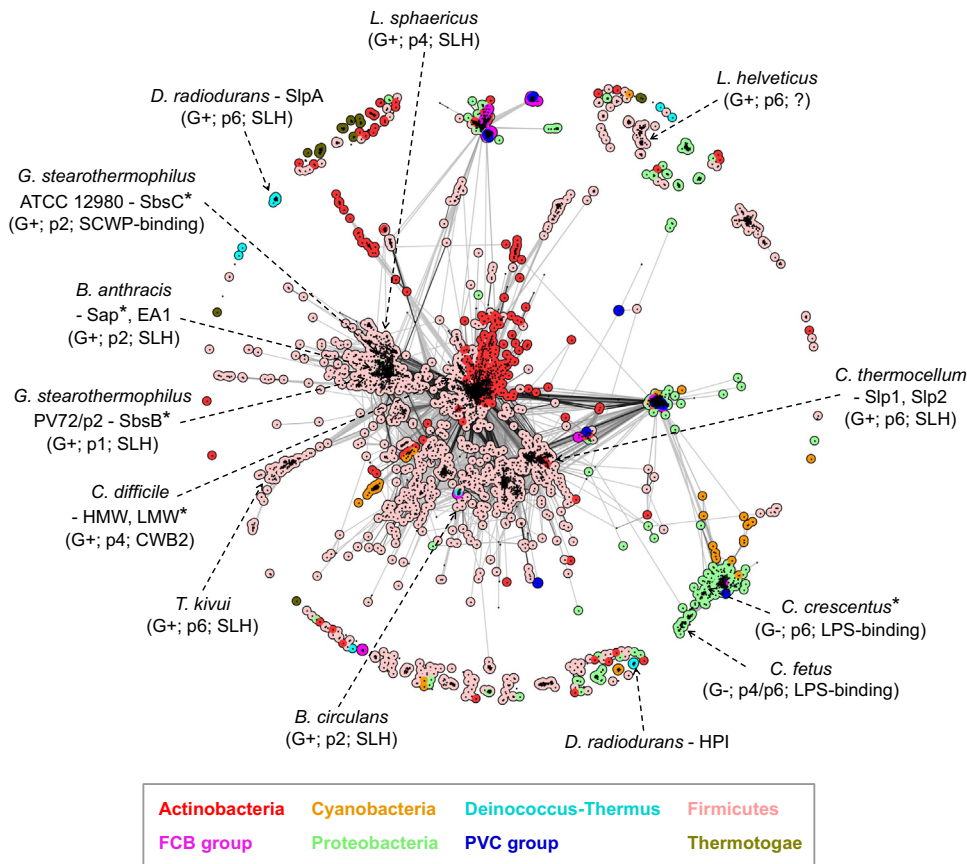
Figure 2. Cluster Map of Bacterial S-layer Proteins. In the same manner as in Figure 1, bacterial S-layer proteins were gathered using BLAST [76] searches and clustered using the CLANS software [77] based on their all-against-all pairwise similarities. Dots represent surface-layer protein (SLP) sequences, and line coloring reflects BLAST *P* values; the darker a line, the lower the *P* value. Colors denote prominent groups of bacteria, shown in the box below the map. Some intensely studied bacterial species are highlighted, with the Gram-type, lattice symmetry, and predicted anchoring sequence shown in brackets (*denotes S-layers with some structural biology data available). Some phyla comprising few representatives in the map, including Acidobacteria, Aquificae, Chloroflexi, and Spirochaetes, are not colored. Notably, some strains of *C. fetus* use SLPs of different molecular weights to form lattices with p4 or p6 symmetry. Abbreviations: *B. anthracis*, *Bacillus anthracis*; *B. circulans*, *Bacillus circulans*; *C. crescentus*, *Caulobacter crescentus*; *C. fetus*, *Campylobacter fetus*; *C. difficile*, *Clostridium difficile*; *C. thermocellum*, *Clostridium thermocellum*; *D. radiodurans*, *Deinococcus radiodurans*; *G. stearothermophilus*, *Geobacillus stearothermophilus*; *L. helveticus*, *Lactobacillus helveticus*; LPS, lipopolysaccharide; *L. sphaericus*, *Lysinibacillus sphaericus*; SLH, S-layer homology domain; *T. kivui*, *Thermoanaerobacter kivui*.

segments in many archaeal SLPs [13,23]. Notably, in some organisms, the lattice-forming and anchoring segments are harbored by two distinct SLPs, for example, in the archaeon *Sulfolobus islandicus* [23]. While the lattice-forming segments are remarkably divergent in their sequences, the anchoring segments show significantly lower sequence variability. They are often even found in SLPs that have otherwise different sequences. Many SLPs of Gram-positive bacteria, for instance, contain three tandem cell-wall-binding S-layer homology (SLH) domains [20].

The comprehensive annotation of the domains of SLPs has largely remained difficult because of their enormous sequence diversity and the lack of homologous domains of known structure. However, the recent structural characterization of many domains of archaeal and bacterial

SLPs suggests that their structural diversity is more limited than previously thought. Most characterized SLP lattice-forming segments are built from the repetition and recombination of a limited set of fold types, with a preponderance of immunoglobulin-like β-sandwich, β-roll, β-helical, and coiled-coil folds [7,16,17,24]. The structural diversity exhibited by the anchoring segments is even more limited; they generally are trimers, pseudo-trimers [20,22,25], or bundles of α-rich folds [18,21], or are single membrane-spanning α-helices [23]. Intriguingly, SLPs contain folds found in eukaryotic cell surface and eukaryotic virus envelope proteins, raising exciting questions on the origin of cell-surface proteins across the different domains of life [24,26].

S-layer Overall Symmetries

S-layers are essentially curved versions of 2D crystals arranged around cells. In general, planar, periodically repeating patterns can be classified according to transformations that leave them invariant, called planar symmetry groups. There are 17 different planar symmetry groups which can be described by translations, rotations, reflections, and glide reflections. Due to limitations imposed by the chiral nature of proteins, including SLPs [27], there are only five general ways of arranging SLPs into a planar crystal with sixfold (p6), fourfold (p4), threefold (p3), twofold (p2), and no rotational symmetry (p1). While hexagonal (p6) symmetries are the most frequently observed arrangement in archaeal and bacterial S-layers, p1, p2, p3, and p4 symmetries are also observed [5,13,28,29]. Based on the symmetry type, the unit cells of S-layer lattices are composed of one to six identical subunits, with the center-to-center spacing between the unit cells ranging from 4 to 35 nm [14]. Consequently, the S-layer lattice is heavily punctuated by uniformly distributed pores of identical size and morphology, covering a majority of the total cell surface area. In many S-layers, two or more different classes of pores, with diameters between 2 and 8 nm, have been observed [14].

Many archaea, in particular members of the phylum Euryarchaeota, which comprise the most laboratory-cultured representative species, possess S-layers with a hexagonal lattice (p6) [13]; examples include *Methanocaldococcus jannaschii*, *Methanothermus fervidus*, *Haloferax volcanii*, and *Halobacterium salinarum*. Unlike Euryarchaeota, Crenarchaeota, which are arguably the next best-studied archaeal phylum, do not have a predominant symmetry type and exhibit lattices with p3 (e.g., *S. islandicus*), p4 (*Staphylothermus marinus*), or p6 (*Pyrobaculum aerophilum*) symmetries. S-layer lattice symmetries of most other archaeal phyla, including Lokiarchaeota, Nanoarchaeota, Thaumarchaeota, and Thorarchaeota, remain sparsely characterized; however, some efforts are being made to characterize these elusive organisms [30].

In comparison to archaea, bacterial S-layers do not show a particular preference for hexagonal symmetries, but instead, show a phylogenetically uncorrelated distribution of p1 (e.g., the Gram-positive firmicute *Geobacillus stearothermophilus* PV72/p2), p2 (the Gram-negative betaproteobacterium *Aquaspirillum putridiconchylium*), p4 (the Gram-positive firmicute *Lysinibacillus sphaericus* CCM2177), and p6 (the Gram-negative alphaproteobacterium *Caulobacter crescentus*) symmetries [5,14,29,31,32]. Notably, some bacteria or their different strains (e.g., *C. fetus* and *G. stearothermophilus* strains) display varying lattice symmetries using different SLPs or different molecular weight species of an SLP [33–36].

S-layer Anchoring on Cells

The envelopes of prokaryotic cells are fundamentally different across bacteria and archaea, and therefore S-layers use vastly different mechanisms for anchoring to cell surfaces (Figure 3). In most archaea, S-layers are attached directly to the cytoplasmic membrane [37,38]. In species of the order Methanobacteriales (e.g., *M. fervidus*), however, the cytoplasmic membrane is surrounded by a cell wall composed of pseudopeptidoglycan, also known as pseudomurein,
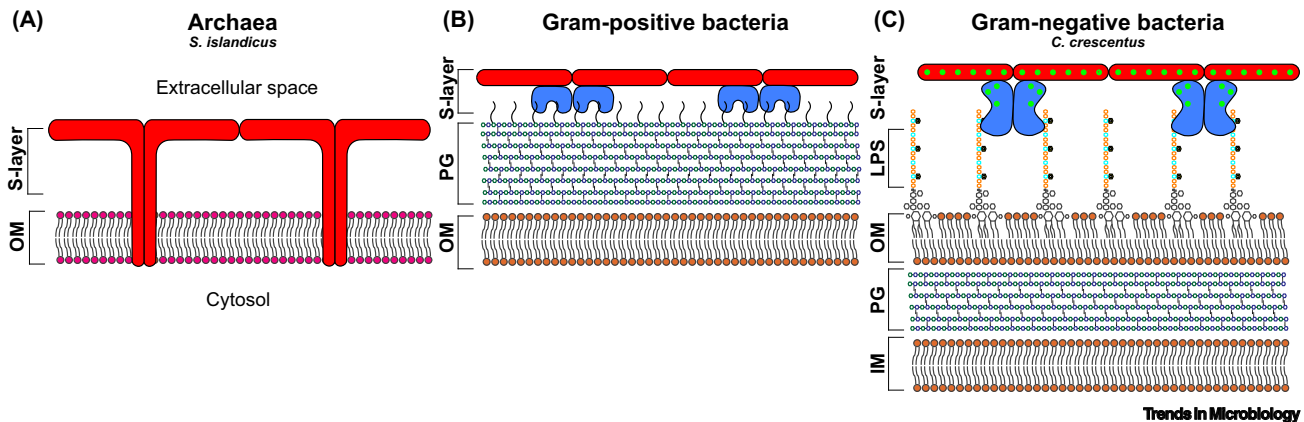
Figure 3. Schematics of Prokaryotic Cell Surfaces. Schematic diagrams of prokaryotic cell surfaces are provided to illustrate the variety of anchoring mechanisms used by S-layers to assemble on cells. (A) Representation of the archaeal cell surface using the crenarchaeon *Sulfolobus islandicus* as an example, experimentally described using high-resolution electron cryotomography (cryo-ET) [23]. Long stalk-like densities of the S-layer are buried within the outer membrane. (B) A generic Gram-positive bacterial outer surface with the S-layer buried within the cell wall. (C) The envelope of the Gram-negative bacterium *Caulobacter crescentus*, as described using cryo-ET [18]. The anchoring domain of the S-layer is noncovalently attached to the O-antigen of LPS. Abbreviations: IM, inner membrane; LPS, lipopolysaccharide; PG, peptidoglycan; OM, outer membrane.

and the S-layer is associated with this pseudomurein layer. While crenarchaeal SLPs, such as those found in the extremophile *S. islandicus*, are generally anchored to the membrane via a C-terminal transmembrane segment [23], most euryarchaeal SLPs appear to be anchored through the covalent attachment of a lipid moiety to their C-terminal end [39–42]. Euryarchaeal SLPs typically contain a C-terminally located tripartite segment that comprises a highly conserved PGF (proline-glycine-phenylalanine) motif, a transmembrane helix, and a cluster of basic residues. In *H. volcanii*, this segment is recognized and cleaved by an archaeosortase (ArtA). Furthermore, ArtA also mediates membrane anchoring of the processed SLP through the attachment of a lipid group. Anchoring mechanisms employed by SLPs of pseudomurein-containing archaea remain unclear, but they presumably, like other archaea, also use their C terminus for anchoring.

Compared with archaea, bacteria exhibit more complex cell wall structures. While Gram-positive bacteria have only a thick peptidoglycan layer surrounding the cytoplasmic or inner membrane (IM), Gram-negative bacteria have a thinner peptidoglycan (PG) layer as well as an outer lipid membrane (OM). In many Gram-positive bacteria, SLPs typically contain three – N- or C-terminally located – tandem repeats of the SLH domain which bind noncovalently to PG-linked pyruvylated secondary cell wall polymers (SCWPs) [20,25,43]. For instance, the SLPs of *B. anthracis* (Sap and EA1) each contain three copies each of the SLH domain at their N terminus, whereas those of *Clostridium thermocellum* (SLAP1 and SLAP2) contain three copies each at their C terminus. Unlike most Gram-positive bacteria, in the majority of clostridial species, such as *C. difficile*, *Clostridium tetani*, and *Clostridium botulinum*, SLPs lack SLH domains and instead contain three tandem repeats of the cell-wall-binding 2 (CWB2) domain, which in *C. difficile* binds to the surface polysaccharide PSII [22,44]. A further anchoring mechanism is exhibited by *G. stearothermophilus* strains, which have five different SLPs, SbsA, SbsB, SbsC, SbsD, and SgsE [5]. While SbsB contains three N-terminal SLH domains, the other four contain three tandem repeats of a third type of SCWP-binding domain. In SbsC, this domain has been shown to interact with a negatively charged SCWP consisting of *N*-acetylglucosamine, glucose, and 2,3-dideoxy-diacetamido mannosamine uronic acid [21]. For some SLPs that lack these anchoring modules, their N or C termini have been implicated in electrostatic interactions with SCWPs. For instance, the C-terminal part of *Lactobacillus acidophilus* ATCC 4356 SlpA is involved in anchoring [45],

whereas *Lactobacillus brevis* ATCC 8287 SlpA uses its N-terminal part [46].

Contrary to Gram-positive bacteria, anchoring mechanisms in Gram-negative bacteria remain less well understood. They do not contain any widespread anchoring domains and appear to use their N or C termini to interact with lipopolysaccharides (LPS) in the outer membrane. In the well studied S-layers of *C. crescentus* and *C. fetus*, the N-terminal segments mediate noncovalent interactions with the O-antigen repeating oligosaccharide of the LPS [18,47]. In fact, a recent study characterized the structural basis of the interaction between *C. crescentus* S-layer and the O-antigen oligosaccharide of LPS [18] and showed that newly synthesized SLPs are guided along the LPS to their final position at the tip of the O-antigen.

Post-translational Modifications of SLPs

In addition to being tremendously diverse in sequence and structure, SLPs display a further level of diversity through post-translational modifications. These modifications are generally species-specific and include cleavage of signal peptides, protein-sorting sequences, or precursor forms; lipidation; glycosylation; and tyrosine phosphorylation [48,49].

Most archaeal and many bacterial SLPs are synthesized with an N- or C-terminal signal peptide (e.g., a bacterial type I secretion signal), a C-terminal sorting signal (e.g., the euryarchaeal PGF-CTERM motif), or occasionally both (e.g., euryarchaeal SLPs typically contain a signal peptide as well as the PGF-CTERM motif). These segments are generally removed following their trans-location across the cytoplasmic membrane [5,13,40,41]. Occasionally, in some organisms, the S-layer is formed by the association of two SLPs obtained by the proteolytic processing of a pre-cursor protein [50,51], for instance, in the bacterium *C. difficile* and the archaeon *S. marinus*.

Another widespread post-translational modification observed in many archaeal and bacterial SLPs is the presence of a wide variety of surface-exposed glycans, covalently linked to specific aspara-gine residues (N-linked glycosylation) or serine/threonine/tyrosine residues (O-linked glycosylation). While both N- and O-linked glycans have been observed in archaeal SLPs, only O-linked glycans have been observed in hitherto characterized bacterial SLPs [5,13,14,52–54]. In recent years, glycosylated SLPs, as well as proteins involved in the synthesis, transport, and linkage of the asso-ciated glycans, have been characterized in several bacteria (e.g., *G. stearothermophilus*) [35,55] and archaea (*H. volcanii*) [56–58]. The role of S-layer glycosylation remains mostly unclear. How-ever, in some organisms, it has been implicated in the stabilization of the S-layer, maintenance of cell shape, adaptation to changing environmental conditions, formation of biofilms, formation of lubricating hydration layers, and modulation of a host immune response.

Protein lipidation is a further type of post-translational modification in which lipid moieties are co-valently linked to proteins. It has been shown to be essential for the attachment of the *H. volcanii* SLP to the cytoplasmic membrane [39,40,42]. Finally, probably the rarest class of post-translational modification observed in SLPs is tyrosine phosphorylation. Thus far, it has been de-scribed only for the SLP of the bacterium *Aeromonas hydrophila* and is involved in lowering its iso-electric point (pI) [59].

Structural Studies of S-layers

There is tremendous excitement in the S-layer field presently, owing to the recent elucidation of several high-resolution X-ray crystallography and electron cryomicroscopy (cryo-EM) structures, which are revolutionizing the field and advancing our understanding of S-layers. In the past, atomic models could not be produced routinely for S-layers due to difficulties associated with electron crystallography, which was the method of choice for studying S-layers [12,60]. In

particular, for S-layers, nanobody-assisted crystallization [61] has allowed researchers to obtain 3D (three-dimensional) crystals of SLPs, leading to atomic structure solution using X-ray crystallography. The cryo-EM resolution revolution [62,63] has further intensified the ability of researchers to produce structures of SLPs. With the advent of powerful techniques such as electron cryotomography (cryo-ET) to solve macromolecular structures [64], structures of S-layers can now be solved directly in their cellular context.

Structures of several S-layer lattice-forming domains have been resolved recently (Figure 4A–D). Taking advantage of the lattice-forming ability of SLPs, an archaeal SLP from *Methanosarcina acetivorans* [24] and a Gram-negative bacterial S-layer from *C. crescentus* [17] were solved using X-ray crystallography. This was made possible by the crystallization of the SLPs into a 3D crystal. In the case of the *C. crescentus* SLP, fortuitous cleavage of the S-layer anchoring domain allowed the S-layer lattice sheets to stack on top of each other [17], leading to the formation of 3D crystals. Nanobody-assisted crystallization circumvents this issue of 2D sheet formation entirely by disrupting the ability of the SLP to form an S-layer lattice. This approach allowed structure determination of the Gram-positive S-layer assembly domains from *G. stearothermophilus* [16] and *B. anthracis* [7]. These new S-layer assembly domain structures (Figure 4A–D) show that these domains are rich in β-strands and form tight lattice structures by initiating multiple contacts along the lattice [17,24].

In addition to lattice formation, SLPs must interact with prokaryotic envelopes to remain anchored to the cell and thereby perform their role at the cell surface. Recently, several structures of S-layer anchoring domains have been reported (Figure 4E–H). The structures of the three aforementioned Gram-positive bacterial anchoring domains, CWB2 [22], SLH [20], and *Geobacillus*

S-layer assembly domains

(A)

Methanosarcina acetivorans
archaeal, PDB ID 3U2H

(B)

Geobacillus stearothermophilus
Gram-positive bacterial, PDB ID 4AQ1

(C)

Bacillus anthracis
Gram-positive bacterial, PDB ID 6HHU

(D)

Caulobacter crescentus
Gram-negative bacterial, PDB ID 5N8P

S-layer anchoring domains

(E)

Clostridium difficile
Gram-positive bacterial, PDB ID 5J6Q
CWB2 domains

(F)

Geobacillus stearothermophilus
Gram-positive bacterial, PDB ID 4UJ6

(G)

Bacillus anthracis
Gram-positive bacterial, PDB ID 3PYW
SLH domains

(H)

Caulobacter crescentus
Gram-negative bacterial, PDB ID 6T72
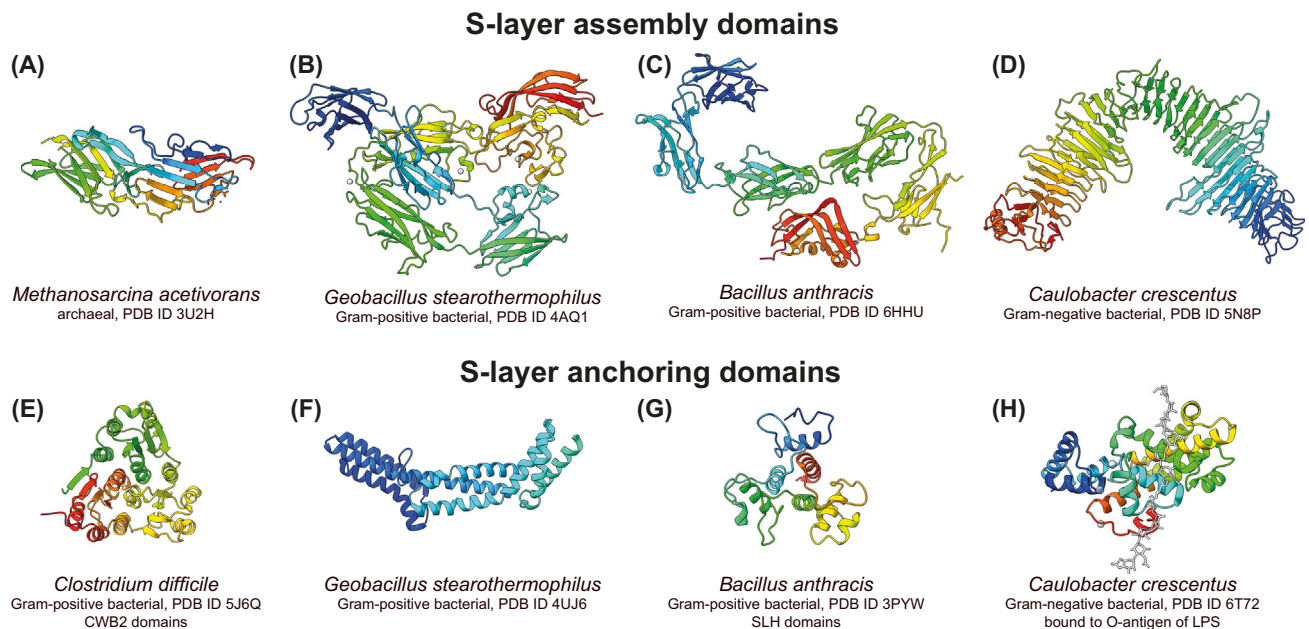bound to O-antigen of LPS

Trends in Microbiology

Figure 4. Structural Biology of Prokaryotic S-Layers. Atomic structures of surface-layer protein (SLP) domains resolved using X-ray crystallography and electron cryomicroscopy (cryo-EM). (A–D) Structures of lattice-forming assembly domains of SLPs. (E–H) Cell-anchoring SLP domains. All figures were made using publicly available atomic coordinates from the protein data bank (PDB) using UCSF ChimeraX [78]. The source organism and the PDB IDs of the structures are indicated below the atomic ribbon diagram colored as rainbow from N to the C terminus.

SCWP-binding domains [21], have been solved with X-ray crystallography revealing predominantly α-helical proteins that interact directly with cell wall components. For Gram-negative bacteria, single-particle cryo-EM was used to solve the structure of the LPS binding domain of the *C. crescentus* SLP, revealing for the first time how the O-antigen is bound noncovalently to the S-layer [18]. No atomic structural data for archaeal anchoring domains are available thus far, and therefore, details of S-layer anchoring on archaeal cells remains poorly understood. Several different mechanisms of anchoring are probably at play in archaea depending on the species, and future structural biology research will be needed to understand in atomic detail how archaeal S-layers are anchored on cells.

Despite recent progress in resolving structures of individual SLP domains, these structures in isolation can rarely explain the architecture and arrangement of the S-layer on cells. Cryo-ET has emerged as an extraordinary tool to solve structures of assembled S-layers *in vitro* or *in situ* on cells [65], providing unprecedented insight into S-layer structural biology. Cryo-ET and cryo-EM
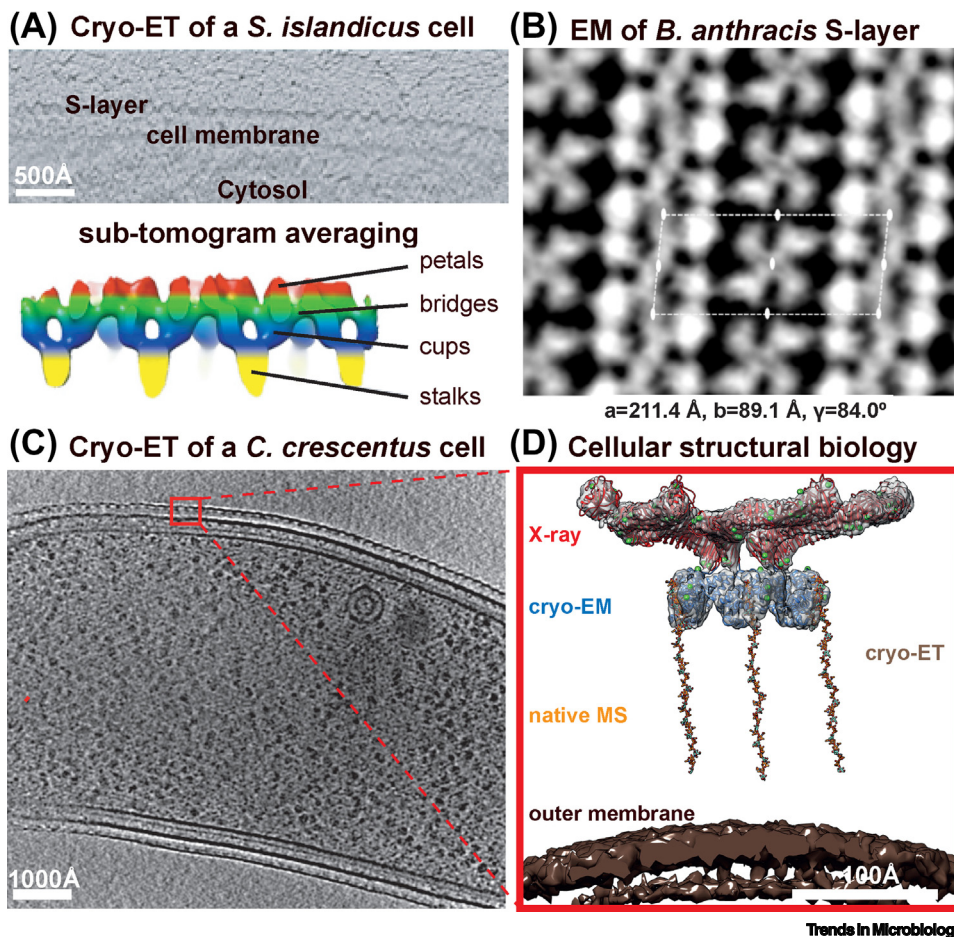

Figure 5. Structural Biology of Assembled S-layers. Examples of high-resolution electron cryomicroscopy (cryo-EM) and electron cryotomography (cryo-ET) analyses of assembled S-layers. (A) Cryo-ET and sub-tomogram averaging of the archaeal S-layer from *Sulfolobus islandicus*. Adapted with permission from Dr Bertram Daum [23]. (B) Cryo-EM projection image of the *Bacillus anthracis* Sap S-layer. Adapted with permission from Prof Han Remaut [7]. (C,D) Cryo-ET and sub-tomogram averaging structure of the S-layer from Gram-negative *Caulobacter crescentus* bacteria bound to the O-antigen of lipopolysaccharide (LPS) [18].

studies can now shed light on how S-layers are assembled on cells (Figure 5), applied to archaeal [23], Gram-positive [7], and Gram-negative bacterial S-layers [18]. Resolutions achievable in cryo-ET are not quite high enough currently; however, potent microscopy and image processing tools [66–69] are beginning to be applied to S-layer structural biology. Using such studies, the relative arrangements of the S-layer assembly and anchoring domains could be discovered in the archaeon *S. islandicus* [23]. In the Gram-negative bacterial S-layer of *C. crescentus*, in addition to the arrangement of the domains, density for the O-antigen of LPS could be observed, proving conclusively that the S-layer is tethered to the cell envelope through noncovalent interactions with the LPS [18].

Common Themes in S-layer Assembly on Prokaryotic Cells

Despite the variation in SLP sequences and structures discussed in this article, and despite the vastly different biochemical properties of envelopes in archaea, Gram-positive, and Gram-negative bacteria, some surprising common themes in S-layer biogenesis have been emerging in recent years [39,70,71]. Using real-time optical microscopy and a variety of strategies to fluorescently tag SLPs, the biogenesis of S-layers could be tracked, for the first time, at high-resolution in some archaea and bacteria, including *H. volcanii*, *C. crescentus*, and *C. difficile* (Fig. 6). These live imaging experiments showed that SLP insertion occurs predominantly at the mid-cell and is probably linked with the cell division and cell elongation machinery of prokaryotes [72]. Although this tantalizing observation has thus far only been reported in a small number of organisms, it perhaps reflects a common and widespread solution to a problem of needing to form a coat on a curved surface, along with the need to form breaks in the lattice for the insertion of new subunits. More research will need to be performed into the molecular cell biology of S-layer biogenesis, to reveal how deep these mechanistic principles are shared across prokaryotes (see Outstanding Questions).

(A) *Haloferax volcanii* archaeal S-layer — 5 μm

(B) *Clostridium difficile* Gram-positive bacterial S-layer — 1 μm

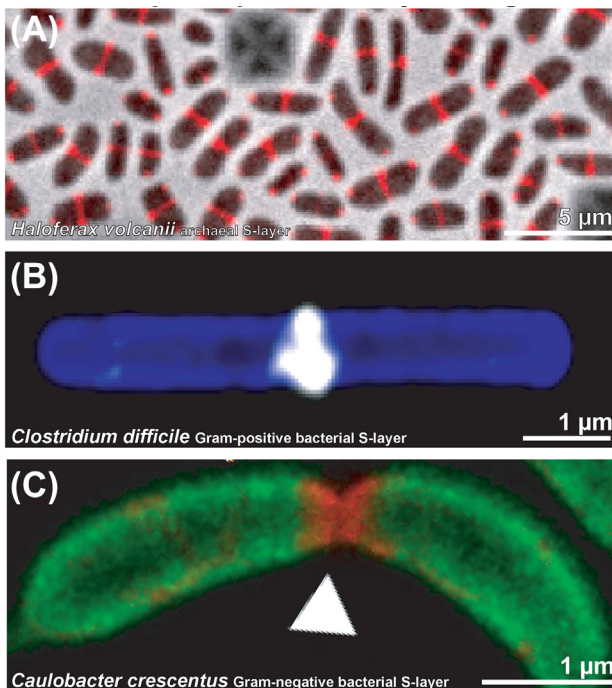**(C)** *Caulobacter crescentus* Gram-negative bacterial S-layer — 1 μm

Figure 6. Mid-cell Surface-Layer Protein (SLP) Insertion Observed across Prokaryotes. (A) Fluorescently tagged SLPs were assembled at the mid-cell of *Haloferax volcanii* archaea [39]. (B) In Gram-positive *Clostridium difficile* bacteria, high-resolution imaging of S-layer assembly revealed similarly directed insertion of new SLP subunits at the mid-cell [71]. (C) Super-resolution imaging of SLP insertion in *Caulobacter crescentus* showed that most SLPs were inserted at the mid-cell, with some insertion observed at the cell poles [70].

Trends in Microbiology

Concluding Remarks

With an increased focus on the structural and cell biology of S-layers, with an ever-increasing focus on archaeal biology [73], together with the immense potential of S-layers in nanotechnology [74,75], and the realization that S-layer biology is a fundamental property of prokaryotes, we anticipate an increased focus on this topic. Novel structural and cell biology techniques will aid our inquiries into S-layer biology, leading to more in-depth insights into these fascinating 2D arrays that assemble on prokaryotic cells with high co-cooperativity. We expect a much greater focus on the fundamental cell-biology mechanisms linking S-layer biogenesis to the prokaryotic cell cycle, and on using SLPs and S-layers to understand post-translational modifications and protein secretion across multiple domains of life.

Outstanding Questions

The most important questions that will drive future research into S-layers are the reasons for similarities in S-layer assembly mechanisms and their regulation with respect to the cell cycle. What is the contribution of divergent and convergent evolution to this process? Can S-layer biology shed light on the evolution of life? Why is S-layer biogenesis coupled so tightly with the prokaryotic cell cycle, with new S-layer insertion predominantly at the mid-cell? Is this the most parsimonious solution to a complex cell biological problem? Armed with tools of modern structural and cell biology, the field is poised to answer these important questions that will not only shed light on a critical aspect of prokaryotic life but will have important implications in the synthesis of novel, biologically inspired nanomaterials.

References

1. Filloux, A. and Whitfield, C. (2016) Editorial: The many wonders of the bacterial cell surface. *FEMS Microbiol. Rev.* 40, 161–163
2. Persat, A. *et al.* (2015) The mechanical world of bacteria. *Cell* 161, 988–997
3. O'Toole, G.A. and Wong, G.C. (2016) Sensational biofilms: surface sensing in bacteria. *Curr. Opin. Microbiol.* 30, 139–146
4. Sleytr, U.B. *et al.* (2019) Crystalline cell surface layers (S-layers) . In *Encyclopedia of Microbiology* (4th edn) (Schmidt, T.M., ed.), pp. 783–792, Academic Press
5. Fagan, R.P. and Fairweather, N.F. (2014) Biogenesis and functions of bacterial S-layers. *Nat. Rev. Microbiol.* 12, 211–222
6. Merrigan, M.M. *et al.* (2013) Surface-layer protein A (SlpA) is a major contributor to host-cell adherence of *Clostridium difficile*. *PLoS One* 8, e78404
7. Fioravanti, A. *et al.* (2019) Structure of S-layer protein Sap reveals a mechanism for therapeutic intervention in anthrax. *Nat. Microbiol.* 4, 1805–1814
8. Pei, Z. and Blaser, M.J. (1990) Pathogenesis of *Campylobacter fetus* infections. Role of surface array proteins in virulence in a mouse model. *J. Clin. Invest.* 85, 1036–1043
9. Blaser, M.J. (1993) Role of the S-layer proteins of *Campylobacter fetus* in serum-resistance and antigenic variation: a model of bacterial pathogenesis. *Am J Med Sci* 306, 325–329
10. Pum, D. *et al.* (2013) S-layer protein self-assembly. *Int. J. Mol. Sci.* 14, 2484–2501
11. Kessel, M. *et al.* (1988) Three-dimensional structure of the regular surface glycoprotein layer of *Halobacterium volcanii* from the Dead Sea. *EMBO J.* 7, 1549–1554
12. Deatherage, J.F. *et al.* (1983) Three-dimensional arrangement of the cell wall protein of *Sulfolobus acidocaldarius*. *J. Mol. Biol.* 167, 823–848
13. Rodrigues-Oliveira, T. *et al.* (2017) Archaeal S-layers: overview and current state of the art. *Front. Microbiol.* 8, 2597
14. Sleytr, U.B. *et al.* (2014) S-layers: principles and applications. *FEMS Microbiol. Rev.* 38, 823–864
15. Avall-Jaaskelainen, S. and Palva, A. (2005) *Lactobacillus* surface layers and their applications. *FEMS Microbiol. Rev.* 29, 511–529
16. Baranova, E. *et al.* (2012) SbsB structure and lattice reconstruction unveil Ca^{2+} triggered S-layer assembly. *Nature* 487, 119–122
17. Bharat, T.A.M. *et al.* (2017) Structure of the hexagonal surface layer on *Caulobacter crescentus* cells. *Nat. Microbiol.* 2, 17059
18. von Kügelgen, A. *et al.* (2020) *In situ* structure of an intact lipopolysaccharide-bound bacterial surface layer. *Cell* 180, 348–358 e15
19. Cohen, S. *et al.* (1991) Nature of the salt dependence of the envelope of a Dead Sea archaebacterium, *Haloferax volcanii*. *Arch. Microbiol.* 156, 198–203
20. Kern, J. *et al.* (2011) Structure of surface layer homology (SLH) domains from *Bacillus anthracis* surface array protein. *J. Biol. Chem.* 286, 26042–26049
21. Pavkov, T. *et al.* (2008) The structure and binding behavior of the bacterial cell surface layer protein SbsC. *Structure* 16, 1226–1237
22. Usenik, A. *et al.* (2017) The CWB2 cell wall-anchoring module is revealed by the crystal structures of the *Clostridium difficile* cell wall proteins Cwp8 and Cwp6. *Structure* 25, 514–521
23. Gambelli, L. *et al.* (2019) Architecture and modular assembly of Sulfolobus S-layers revealed by electron cryotomography. *Proc. Natl. Acad. Sci. U. S. A.* 116, 25278–25286
24. Arbing, M.A. *et al.* (2012) Structure of the surface layer of the methanogenic archaean *Methanosarcina acetivorans*. *Proc. Natl. Acad. Sci. U. S. A.* 109, 11812–11817
25. Blackler, R.J. *et al.* (2018) Structural basis of cell wall anchoring by SLH domains in *Paenibacillus alvei*. *Nat. Commun.* 9, 3120
26. Jing, H. *et al.* (2002) Archaeal surface layer proteins contain beta propeller, PKD, and beta helix domains and are related to metazoan cell surface proteins. *Structure* 10, 1453–1464
27. Rupp, B. (2009) *Biomolecular Crystallography: Principles, Practice, and Application to Structural Biology*, CRC Press
28. Sleytr, U.B. *et al.* (1996) *Crystalline Bacterial Cell Surface Proteins*, Elsevier Science
29. Sára, M. and Sleytr, U.B. (2000) S-layer proteins. *J. Bacteriol.* 182, 859–868
30. Li, P.N. *et al.* (2018) Nutrient transport suggests an evolutionary basis for charged archaeal surface layer proteins. *ISME J.* 12, 2389–2402
31. Beveridge, T.J. and Graham, L.L. (1991) Surface layers of bacteria. *Microbiol. Rev.* 55, 684–705
32. Chung, S. *et al.* (2010) Self-catalyzed growth of S layers via an amorphous-to-crystalline transition limited by folding kinetics. *Proc. Natl. Acad. Sci. U. S. A.* 107, 16536–16541
33. Fujimoto, S. *et al.* (1991) Correlation between molecular size of the surface array protein and morphology and antigenicity of the *Campylobacter fetus* S layer. *Infect. Immun.* 59, 2017–2022
34. Sára, M. and Sleytr, U.B. (1994) Comparative studies of S-layer proteins from *Bacillus stearothermophilus* strains expressed during growth in continuous culture under oxygen-limited and non-oxygen-limited conditions. *J. Bacteriol.* 176, 7182–7189

35. Schaffer, C. *et al.* (2002) The surface layer (S-layer) glycoprotein of *Geobacillus stearothermophilus* NRS 2004/3a. Analysis of its glycosylation. *J. Biol. Chem.* 277, 6230–6239

36. Egelseer, E.M. *et al.* (2001) Characterization of an S-layer glycoprotein produced in the course of S-layer variation of *Bacillus stearothermophilus* ATCC 12980 and sequencing and cloning of the sbsD gene encoding the protein moiety. *Arch. Microbiol.* 177, 70–80

37. Klingl, A. (2014) S-layer and cytoplasmic membrane – exceptions from the typical archaeal cell wall with a focus on double membranes. *Front. Microbiol.* 5, 624

38. Pohlschroder, M. *et al.* (2018) Archaeal cell surface biogenesis. *FEMS Microbiol. Rev.* 42, 694–717

39. Abdul-Halim, M.F. *et al.* (2020) Lipid anchoring of archaeosortase substrates and midcell growth in Haloarchaea. *mBio* 11, e00349-20

40. Abdul Halim, M.F. *et al.* (2015) Permuting the PGF signature motif blocks both archaeosortase-dependent C-terminal cleavage and prenyl lipid attachment for the *Haloferax volcanii* S-layer glycoprotein. *J. Bacteriol.* 198, 808–815

41. Haft, D.H. *et al.* (2012) Archaeosortases and exosortases are widely distributed systems linking membrane transit with post-translational modification. *J. Bacteriol.* 194, 36–48

42. Konrad, Z. and Eichler, J. (2002) Lipid modification of proteins in Archaea: attachment of a mevalonic acid-based lipid moiety to the surface-layer glycoprotein of *Haloferax volcanii* follows protein translocation. *Biochem. J.* 366, 959–964

43. Mesnage, S. *et al.* (2000) Bacterial SLH domain proteins are non-covalently anchored to the cell surface via a conserved mechanism involving wall polysaccharide pyruvylation. *EMBO J.* 19, 4473–4484

44. Willing, S.E. *et al.* (2015) *Clostridium difficile* surface proteins are anchored to the cell wall using CWB2 motifs that recognise the anionic polymer PSII. *Mol. Microbiol.* 96, 596–608

45. Smit, E. *et al.* (2001) The S-layer protein of *Lactobacillus acidophilus* ATCC 4356: identification and characterisation of domains responsible for S-protein assembly and cell wall binding. *J. Mol. Biol.* 305, 245–257

46. Avall-Jaaskelainen, S. *et al.* (2008) Identification and characterization of domains responsible for self-assembly and cell wall binding of the surface layer protein of *Lactobacillus brevis* ATCC 8287. *BMC Microbiol.* 8, 165

47. Dworkin, J. *et al.* (1995) A lipopolysaccharide-binding domain of the *Campylobacter fetus* S-layer protein resides within the conserved N terminus of a family of silent and divergent homologs. *J. Bacteriol.* 177, 1734–1741

48. Macek, B. *et al.* (2019) Protein post-translational modifications in bacteria. *Nat. Rev. Microbiol.* 17, 651–664

49. Eichler, J. and Adams, M.W. (2005) Posttranslational protein modification in Archaea. *Microbiol. Mol. Biol. Rev.* 69, 393–425

50. Bradshaw, W.J. *et al.* (2018) The structure of the S-layer of *Clostridium difficile*. *J. Cell Commun. Signal.* 12, 319–331

51. Peters, J. *et al.* (1996) Hyperthermostable surface layer protein tetrabrachion from the archaebacterium *Staphylothermus marinus*: evidence for the presence of a right-handed coiled coil derived from the primary structure. *J. Mol. Biol.* 257, 1031–1041

52. Kandiba, L. and Eichler, J. (2014) Archaeal S-layer glycoproteins: post-translational modification in the face of extremes. *Front. Microbiol.* 5, 661

53. Lu, H. *et al.* (2020) Agl22 and Agl23 are involved in the synthesis and utilization of the lipid-linked intermediates in the glycosylation pathways of the halophilic archaeaon *Haloarcula hispanica*. *Mol. Microbiol.* Published online July 24, 2020. https://doi.org/10.1111/mmi.14577

54. Schaffer, C. and Messner, P. (2017) Emerging facets of prokaryotic glycosylation. *FEMS Microbiol. Rev.* 41, 49–91

55. Schuster, B. and Sleytr, U.B. (2015) Relevance of glycosylation of S-layer proteins for cell surface properties. *Acta Biomater.* 19, 149–157

56. Tamir, A. and Eichler, J. (2017) N-glycosylation is important for proper *Haloferax volcanii* S-layer stability and function. *Appl. Environ. Microbiol.* 83, e03152-16

57. Rodrigues-Oliveira, T. *et al.* (2019) Environmental factors influence the *Haloferax volcanii* S-layer protein structure. *PLoS One* 14, e0216863

58. Shalev, Y. *et al.* (2018) Comparative analysis of surface layer glycoproteins and genes involved in protein glycosylation in the genus *Haloferax*. *Genes (Basel)* 9, 172

59. Thomas, S.R. and Trust, T.J. (1995) Tyrosine phosphorylation of the tetragonal paracrystalline array of *Aeromonas hydrophila*: molecular cloning and high-level expression of the S-layer protein gene. *J. Mol. Biol.* 245, 568–581

60. Lupas, A. *et al.* (1994) Domain structure of the *Acetogenium kivui* surface layer revealed by electron crystallography and sequence analysis. *J. Bacteriol.* 176, 1224–1233

61. Uchanski, T. *et al.* (2020) Nanobodies to study protein conformational states. *Curr. Opin. Struct. Biol.* 60, 117–123

62. Cheng, Y. (2018) Single-particle cryo-EM-How did it get here and where will it go. *Science* 361, 876–880

63. Kühlbrandt, W. (2014) Biochemistry. The resolution revolution. *Science* 343, 1443–1444

64. Briggs, J.A. (2013) Structural biology *in situ* – the potential of subtomogram averaging. *Curr. Opin. Struct. Biol.* 23, 261–267

65. Böhning, J. and Bharat, T.A.M. (2020) Towards high-throughput *in situ* structural biology using electron cryotomography. *Prog. Biophys. Mol. Biol.* Published online June 21, 2020. https://doi.org/10.1016/j.pbiomolbio.2020.05.010

66. Turoňová, B. *et al.* (2017) Efficient 3D-CTF correction for cryo-electron tomography using NovaCTF improves subtomogram averaging resolution to 3.4Å. *J. Struct. Biol.* 199, 187–195

67. Fernandez, J.J. *et al.* (2018) Cryo-tomography tilt-series alignment with consideration of the beam-induced sample motion. *J. Struct. Biol.* 202, 200–209

68. Navarro, P.P. *et al.* (2018) Protocols for subtomogram averaging of membrane proteins in the dynamo software package. *Front. Mol. Biosci.* 5, 82

69. Himes, B.A. and Zhang, P. (2018) emClarity: software for high-resolution cryo-electron tomography and subtomogram averaging. *Nat. Methods* 15, 955–961

70. Comerci, C.J. *et al.* (2019) Topologically-guided continuous protein crystallization controls bacterial surface layer self-assembly. *Nat. Commun.* 10, 2731

71. Oatley, P. *et al.* (2020) Spatial organization of *Clostridium difficile* S-layer biogenesis. *Sci. Rep.* 10, 14089

72. Zink, I.A. *et al.* (2019) CRISPR-mediated gene silencing reveals involvement of the archaeal S-layer in cell division and virus infection. *Nat. Commun.* 10, 4797

73. Eme, L. *et al.* (2017) Archaea and the origin of eukaryotes. *Nat. Rev. Microbiol.* 15, 711–723

74. Schuster, B. and Sleytr, U.B. (2020) Nanotechnology with S-layer proteins. *Methods Mol. Biol.* 2073, 195–218

75. Charrier, M. *et al.* (2019) Engineering the S-layer of *Caulobacter crescentus* as a foundation for stable, high-density, 2D living materials. *ACS Synth. Biol.* 8, 181–190

76. Camacho, C. *et al.* (2009) BLAST+: architecture and applications. *BMC Bioinform.* 10, 421

77. Frickey, T. and Lupas, A. (2004) CLANS: A Java application for visualizing protein families based on pairwise similarity. *Bioinformatics* 20, 3702–3704

78. Goddard, T.D. *et al.* (2018) UCSF ChimeraX: Meeting modern challenges in visualization and analysis. *Protein Sci.* 27, 14–25